AGU PUBLICATIONS

Geophysical Research Letters

RESEARCH LETTER
10.1002/2017GL074594

Key Points:
- Both ice and marine sediment core data support a major nonuniform retreat of Antarctic sea ice during the early last interglacial
- The 128 ka sea ice retreat was largest in the Atlantic and smallest in the Pacific sector of the Southern Ocean
- The spatial pattern of $\delta^{18}O$ across Antarctica is sensitive to the spatial pattern of sea ice retreat

Supporting Information:
- Supporting Information S1

Correspondence to:
M. D. Holloway,
maxllo15@bas.ac.uk

Citation:
Holloway, M. D., Sime, L. C., Allen, C. S., Hillenbrand, C.-D., Bunch, P., Wolff, E., & Valdes, P. J. (2017). The spatial structure of the 128 ka Antarctic sea ice minimum. *Geophysical Research Letters*, *44*, 11,129–11,139. https://doi.org/10.1002/2017GL074594

Received 15 JUN 2017
Accepted 12 OCT 2017
Accepted article online 18 OCT 2017
Published online 11 NOV 2017

The Spatial Structure of the 128 ka Antarctic Sea Ice Minimum

Max D. Holloway[1,2], Louise C. Sime[1], Claire S. Allen[1], Claus-Dieter Hillenbrand[1], Pete Bunch[3], Eric Wolff[4], and Paul J. Valdes[2]

[1]British Antarctic Survey, Cambridge, UK, [2]School of Geographical Sciences, University of Bristol, Bristol, UK, [3]Department of Engineering, University of Cambridge, Cambridge, UK, [4]Department of Earth Sciences, University of Cambridge, Cambridge, UK

Abstract We compare multi-ice core data with $\delta^{18}O$ model output for the early last interglacial Antarctic sea ice minimum. The spatial pattern of $\delta^{18}O$ across Antarctica is sensitive to the spatial pattern of sea ice retreat. Local sea ice retreat increases the proportion of winter precipitation, depleting $\delta^{18}O$ at ice core sites. However, retreat also enriches $\delta^{18}O$ because of the reduced source-to-site distance for atmospheric vapor. The joint overall effect is for $\delta^{18}O$ to increase as sea ice is reduced. Our data-model comparison indicates a winter sea ice retreat of 67, 59, and 43% relative to preindustrial in the Atlantic, Indian, and Pacific sectors of the Southern Ocean. A compilation of Southern Ocean sea ice proxy data provides weak support for this reconstruction. However, most published marine core sites are located too far north of the 128,000 years B.P. sea ice edge, preventing independent corroboration for this sea ice reconstruction.

Plain Language Summary The Antarctic isotope and temperature maximum, which occurred approximately 128,000 years before present (B.P.) during the warmer than present last interglacial period, is associated with a major retreat of Antarctic sea ice. Understanding the details of this major sea ice retreat is crucial in order to understand the sensitivity of the Southern Hemisphere sea ice system and to evaluate the performance of climate model simulations in response to future warming. This work uses a multi-ice and ocean core data-model evaluation to assess the magnitude and spatial pattern of this sea ice retreat. Our results suggest that sea ice retreat was greatest in the Atlantic and Indian sectors of the Southern Ocean and less in the Pacific sector. These results may have had serious implications for the stability of marine terminating glaciers around the Antarctic Ice Sheet and their contribution to the last interglacial sea level rise. These results also support a hypothesized slowdown in northward ocean heat transport during the early last interglacial.

1. Introduction

Sea ice is an important amplifier in the climate system, affecting the surface energy budget by reflecting incoming solar radiation and regulating the exchange of heat and CO_2 between the atmosphere and ocean. Compared with the Northern Hemisphere, there is lower confidence in predictions of Southern Hemisphere sea ice change; but predictions of environmental and climate change across the Southern Hemisphere are dependent on sea ice parameters (Intergovernmental Panel on Climate Change (IPCC), 2013). Our understanding of the long-term (i.e., beyond the satellite era) interplay between sea ice and the climate system can be improved by examining how sea ice responded during a range of past climates (de Vernal et al., 2013; Goosse et al., 2013; Roche et al., 2012).

During the last interglacial (LIG; 130,000 to 115,000 years ago), polar (Capron et al., 2014; Jouzel et al., 2007; Masson-Delmotte et al., 2011) and perhaps global (Hoffman et al., 2017) temperatures were warmer than today. The LIG thus allows investigation of the sea ice response to warmer than present conditions. Additionally, compared to prior warm intervals, the amount of paleoclimate data from the LIG period is larger (Bakker et al., 2014; Capron et al., 2014). Combining climate model simulations with paleoclimate data over this period thus provides a useful opportunity to gain insight into climate processes and feedbacks during periods of past warmth.

Ice core stable water isotope ($\delta^{18}O$ and δD) records from East Antarctica show an isotopic maximum, associated with peak Antarctic warmth, around 128,000 years ago (128 ka), that is, early in the LIG. The $\delta^{18}O$

maximum is +2 to +4‰ higher than during the last 3 ka, suggesting a significantly warmer Antarctic climate at 128 ka. Recent work demonstrated that this early LIG Antarctic isotopic maximum may be due to a major reduction in Antarctic winter sea ice cover (Holloway, Sime, Singarayer, Tindall, Bunch, et al., 2016). This hypothesis is supported by sea salt flux records from the European Project for Ice Coring in Antarctica (EPICA) Dome C (EDC) and EPICA Dronning Maud Land (EDML) ice cores, which are interpreted as a proxy of past sea ice extent (Abram et al., 2013; Fischer et al., 2007; Levine et al., 2014; Wolff et al., 2010). These records display a minimum in sea salt flux around 128 ka, suggesting major sea ice retreat in both the Atlantic and Indian sectors of the Southern Ocean at this time (Fischer et al., 2007; Wolff et al., 2010, 2006). However, a sea salt record from the Talos Dome ice core (TALDICE) suggests little or no LIG sea ice retreat in the Pacific sector of the Southern Ocean when compared to the Holocene (Schüpbach et al., 2013). Additionally, although marine sediment cores are often located too far north to inform on interglacial sea ice changes (e.g., Capron et al., 2014), some qualitative sea ice reconstructions are consistent with reduced Antarctic winter sea ice extent during the peak LIG compared to the modern and Late Holocene (Crosta et al., 2004; Esper & Gersonde, 2014a; Gersonde & Zielinski, 2000; Schneider-Mor et al., 2012).

A bipolar-seesaw warming of the Southern Ocean after the penultimate glacial termination (Deaney et al., 2017; Govin et al., 2015; Marino et al., 2015) provides a possible explanation for the sea ice retreat. This interpretation is also consistent with data suggesting an average of +2°C warmer sea surface temperatures during the early LIG (Capron et al., 2014). Holloway, Sime, Singarayer, Tindall, Bunch, et al. (2016) calculated the most likely maximum reduction in winter sea ice area using LIG Antarctic isotope data from four ice cores. However, they did not attempt to look at the most likely spatial structure of the sea ice retreat. Information on spatial structure will help to better understand the retreat and its causes.

It is possible to use ice core data to examine the spatial structure since less extensive sea ice permits greater transfer of heat and moisture inland and leads to less negative $\delta^{18}O$ (Holloway, Sime, Singarayer, Tindall, Bunch, et al., 2016; Noone & Simmonds, 2004). Therefore, a multi-ice core analysis, in conjunction with isotope-enabled general circulation model (GCM) experiments, can provide information about the configuration of past Antarctic sea ice (Noone & Simmonds, 2004). Because absolute changes in sea ice extent are largest during the winter (September) sea ice maximum, we focus our examination on changes during this season.

Here we evaluate isotope-enabled GCM experiments against Antarctic ice core records covering the LIG to (i) examine the mechanisms that link changes in Antarctic sea ice extent and the pattern of $\delta^{18}O$ across the Antarctic Ice Sheet and (ii) evaluate the spatial structure of the sea ice retreat. We test simulated sea ice retreat scenarios against ice core isotopic data and compare the results against sea ice constraints from proxy data of marine sediment cores spanning the LIG.

2. Methods

2.1. Climate Model Experiments

We carry out a series of isotope-enabled HadCM3 (Holloway, Sime, Singarayer, Tindall & Valdes, 2016; Tindall et al., 2009) GCM experiments. Various scenarios are investigated by forcing a Southern Ocean sea ice retreat using a positive heat flux applied to the underside of sea ice. This enables different magnitudes and spatial patterns of sea ice retreat to be forced, while ensuring as far as possible that the simulation remains physically consistent. Using this method, the sea ice evolves with the coupled model, growing and retreating seasonally, and the ocean and atmosphere respond to sea ice changes as expected.

We perform an ensemble of experiments using 128 ka boundary conditions, following Holloway, Sime, Singarayer, Tindall, Bunch, et al. (2016); orbital parameters are taken from Berger and Loutre (1991), atmospheric CO_2 is derived from the Vostok ice core (Loulergue et al., 2008; Petit et al., 1999), and CH_4 and N_2O are from the EPICA Dome C ice core (Spahni et al., 2005). No change is applied to the Antarctic Ice Sheet configuration. A control experiment was forced by 128 ka orbital and greenhouse gas forcing alone, with no additional forcing applied to the sea ice. This experiment was run for 700 years. After this time it had reached quasi-equilibrium with the prescribed boundary conditions (drifts in the surface and middepth ocean were negligible). All subsequent sea ice retreat experiments were continued from the end of this 128 ka control experiment for an additional 50 years—with prescribed sea ice forcing as described below. The sea ice response reached an equilibrium with the input heat flux within 20 years of each simulation, so the final 30 years was used in the subsequent analyses.

The first suite of sea ice retreat experiments included a uniform retreat (hereafter referred to as "uniform") with sea ice being reduced at all longitudes of the Southern Ocean (following the approach described in Holloway, Sime, Singarayer, Tindall, Bunch, et al., 2016). The next suite of experiments included an idealized spatially constrained sea ice retreat. We split the Southern Ocean into two sectors spanning 180° longitude each and then forced sea ice retreat in one sector by applying a heat flux of 80 W m^{-2} while applying only 20 W m^{-2} to the other sector.

A final suite of sea ice retreat experiments considered a range of "realistic" scenarios, whereby different magnitudes of sea ice retreat were applied to the Atlantic (defined as longitudes between 70°W and 20°E), Pacific (150°E–70°W), and/or Indian (20°E–150°E) sectors of the Southern Ocean.

To aid the comparison with Antarctic ice core data, simulated $\delta^{18}O$ output from 90 to 60°S was regridded to an equal area 50 km grid and smoothed with the surrounding 100 km in order to minimize any grid dependence near the pole (Sime et al., 2008). Simulated anomalies were calculated relative to a 800 year long preindustrial experiment, forced by 1,850 years B.P. orbit and greenhouse gas concentrations (CO_2 is 280 ppmv; CH_4 is 760 ppbv; and N_2O is 270 ppbv).

2.2. Ice Core Data

Model output was compared against five published ice core records from East Antarctica (Masson-Delmotte et al., 2011); Vostok (Petit et al., 1999), Dome F (DF) (Kawamura et al., 2007), EDC (Jouzel et al., 2007), EDML (EPICA Community Members, 2006), and TALDICE (Stenni et al., 2011). Fractional isotopic content is expressed for oxygen-18 (in ‰) as

$$\delta^{18}O = 1{,}000 \times \left[\left(H_2^{18}O/H_2^{16}O\right)/R_{VSMOW} - 1\right], \quad (1)$$

where R_{VSMOW} is the ratio of $H_2^{18}O$ to $H_2^{16}O$ for Vienna standard mean ocean water (VSMOW). The ice core isotope records were synchronized to the EDC3 age scale (Parrenin et al., 2007) and interpolated onto a common 100 year time grid. In order to minimize the effect of residual temporal misalignment between the ice cores, a 1,500 year low-pass filter was applied to each record before taking the LIG peak (Sime et al., 2009). The misalignment and isotope measurement error were assumed to be negligible after this averaging. The EDC3 age scale was chosen because the version of the EDML record corrected for upstream altitude changes and for the changing $\delta^{18}O$ ratio of seawater is not available on the more recent AICC2012 age scale. However, as the two age models are less than 700 years apart at 128 ka and because we were only interested in the LIG $\delta^{18}O$ maximum across ice core records, the 128 ka snapshots carried out here remain appropriate. $\delta^{18}O$ anomalies are calculated relative to the last 3,000 years.

2.3. Marine Sediment Core Data

We compiled proxy data from published records from the Southern Ocean (Table 1) that include direct proxy data for winter and summer sea ice presence and summer sea surface temperature (SSST) reconstructions for the LIG (see supporting information; Becquey & Gersonde, 2002, 2003; Benz et al., 2016; Bianchi & Gersonde, 2002; Bohrmann, 1999; Brathauer & Abelmann, 1999; Brathauer et al., 2001; Crosta et al., 1998, 2004; Esper & Gersonde, 2014a, 2014b; Frank et al., 1996, 1999, 2000; Gersonde et al., 2003, 2005; Gersonde & Ott, 1997; Gersonde & Zielinski, 2000; Hodell et al., 2003; Mackensen, 2001; Moore et al., 1999; Mulitza et al., 1999; Niebler, 1995, 2004; Nürnberg et al., 1997; Pichon et al., 1992; Pugh et al., 2009; Schneider-Mor et al., 2005, 2008, 2012; Waelbroeck et al., 2009; Zielinski et al., 2002, 1998). Although only the southernmost LIG records may provide direct evidence of sea ice cover suitable for a comparison with the model results, the SSST estimates from locations farther North still add valuable context to the Southern Ocean conditions during the LIG. For comparison with model outputs, we assumed that the minimum sea ice extent coincided with peak SSSTs and the peak oxygen isotope anomaly in the Antarctic ice cores (Holloway, Sime, Singarayer, Tindall, Bunch, et al., 2016). The marine core sites with the sea ice and SSST data were assigned to seven simplified classes that reflect prominent oceanographic boundaries and ecological regions that are well defined by/represented in the sea ice and SSST proxies: 0 = north of the maximum winter sea ice extent, SSST > 3°C; 1 = north of the maximum winter sea ice extent, no information on SSST; 2 = north of the maximum winter sea ice extent, SSST < 3°C; 3 = at or south of the maximum winter sea ice extent; 4 = at or south of the average winter sea ice extent; 5 = at or south of the maximum summer sea ice extent; and 6 = at or south of the average summer sea ice extent.

The agreement between the modern oceanographic setting and the classification of the sediment core sites based on the modern proxy classification (supporting information Figure S1) gives confidence that our sea

Table 1
Marine Sediment Core Records

Core	Latitude	Longitude	Sector	LIG classification	Modern classification
SO136-111	−56.667	160.223	West Pacific	0	0
MD 84 551	−55.01	73.17	Central Indian	0	2
PS2603-3	−53.986	37.628	SW Indian	0	2
ODP 1094	−53.18	5.13	SE Atlantic	0	2
PS2102-2	−53.073	−4.986	SE Atlantic	0	2
ODP 1093	−49.976	5.865	SE Atlantic	0	0
PS1778-5	−49.012	−12.080	SE Atlantic	0	0
PS2498-1	−44.153	−14.228	Central S Atlantic	0	0
PS58/271-1	−61.243	−116.047	Central S Pacific	0	0
PS1768-8	−52.593	4.475	SE Atlantic	0	2
PS2276-4	−54.635	−23.952	Central S Atlantic	2	2
PS1772-8	−55.458	1.163	SE Atlantic	0	3
PS1649-2	−54.910	3.306	SE Atlantic	1	3
PS1652-2	−53.663	5.098	SE Atlantic	1	3
PS2499-5	−46.512	−15.333	Central S Atlantic	1	0
PS2305-6	−58.720	−33.036	Central S Atlantic	3	4

Note. ID and location (latitude, longitude, and Southern Ocean sector) of marine sediment core sites with the classification of sea ice cover and summer sea surface temperature (SSST) for the modern and reconstructed for the peak LIG. Reconstructed sea ice and SSST conditions are quantified using a scale from 0 (north of the maximum winter sea ice) to 6 (at or south of the average summer sea ice extent). See section 2.3 for full details of the classification and supporting information Table S1 for full details of the records.

ice and SSST proxy data compilation is reliable. Supporting information Text S1 gives full details of the compiled marine core records, including chronological methods and the proxies used to derive quantitative, semiquantitative, and/or qualitative estimates of sea ice cover and SSST.

3. Results

3.1. Idealized Sea Ice Forcing Experiments

While there is a weak response to 128 ka orbital and greenhouse gas forcing alone (Figure 1a), a uniform sea ice retreat can increase δ^{18}O by around 2–4‰ across Antarctica (Figure 1b) (Holloway, Sime, Singarayer, Tindall, Bunch, et al., 2016; Noone & Simmonds, 2004). These δ^{18}O anomalies are significant beyond internal model variability (supporting information Text S2 and Figure S2; Schurer et al., 2014). At the ice core sites, δ^{18}O is enriched by 0.5, 0.5, 0.7, 0.8, and 0.8‰ per 10% retreat of winter sea ice area at DF, EDC, EDML, Vostok, and TALDICE, respectively. A Bayesian multivariate linear regression (see Holloway, Sime, Singarayer, Tindall, Bunch, et al., 2016) to calculate the best fit uniform winter sea ice retreat including the TALDICE ice core data (not included in the Holloway, Sime, Singarayer, Tindall, Bunch, et al. (2016) calculation) suggests that a spatially uniform reduction in winter sea ice area of 61% (Figure 1b) best explains the 128 ka isotope maximum (95% credible interval for any one year of [54%, 68%]). This estimate is lower than the 65% estimated by Holloway, Sime, Singarayer, Tindall, Bunch, et al. (2016) because the TALDICE record shows lower peak δ^{18}O values at 128 ka relative to the other ice cores. This highlights the need for more and more widespread ice core data covering the LIG to improve the robustness of LIG climate assessments. A uniform 61% retreat of winter sea ice area produces a root-mean-square error (RMSE) between simulated and observed ice core δ^{18}O anomalies of 0.87‰.

When sea ice retreat is nonuniform, δ^{18}O tends to be more enriched closer to the regions of greater sea ice retreat (Figures 1c and 1d). This significantly influences the spatial pattern of δ^{18}O anomalies across the five ice core sites but has little effect on the zonal mean δ^{18}O response or the total magnitude of winter sea ice reduction. There are significant differences in the model-data δ^{18}O agreement depending on the spatial pattern of sea ice retreat. Greater sea ice retreat in the Ross Sea sector (Figure 1d) significantly worsens the model-data

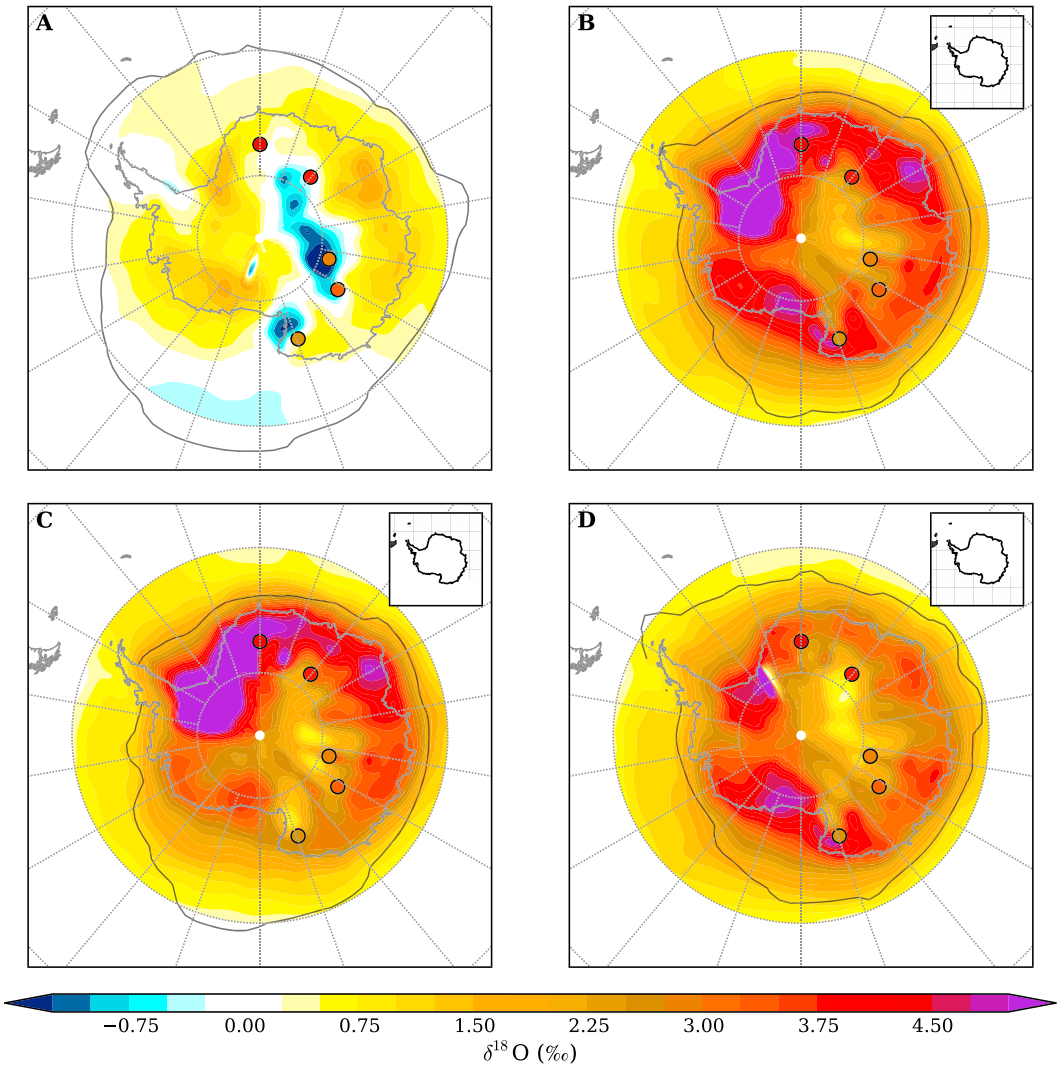

Figure 1. Spatial pattern of δ^{18}O anomalies. Precipitation weighted δ^{18}O anomalies (LIG-PI) for 128 ka simulations with (a) no sea ice retreat forcing, (b) a uniform 61% retreat of the winter sea ice area, (c) more sea ice retreat between 60°W and 120°E ("Weddell Sea sector"), and (d) more sea ice retreat between 120°E and 60°W ("Ross Sea sector"). Filled circles show ice core δ^{18}O anomalies at ice core sites for the LIG peak (128 ± 0.75 ka). Grey lines signify the 15% September sea ice concentration threshold. Insets show the corresponding region where largest heat fluxes (greatest sea ice retreat) were applied.

agreement, increasing the RMSE to 1.76‰. In contrast, less sea ice in the Weddell Sea sector (Figure 1c) provides an identical RMSE as the best fit uniform scenario of 0.87‰; even though the Weddell Sea sector experiment results in 7% less total winter sea ice retreat (54%) compared to the best fit uniform scenario, it provides an equal match to the ice core data. The data therefore allow equally for a uniform retreat or for greater retreat in the Weddell Sea region but make it unlikely that there was greater retreat in other regions.

We decomposed simulated δ^{18}O changes (supporting information Figures S3a, S3d, and S3g) into those due to changes in the seasonal cycle of precipitation (supporting information Figures S3b, S3e, and S3h) and those due to changes in the isotopic composition of monthly precipitation (supporting information Figures S3c, S3f, and S3i) (Holloway, Sime, Singarayer, Tindall, Bunch, et al., 2016; Liu & Battisti, 2015). These two mechanisms have opposing contributions to the total δ^{18}O change. First, for all cases of sea ice retreat there is a shift in the proportion of precipitation toward colder months, which lowers δ^{18}O. Intuitively, this is as expected; the absolute decrease in sea ice extent is mainly a result of less sea ice expansion during winter, allowing more water vapor to reach central Antarctica and increasing the proportion of winter precipitation.

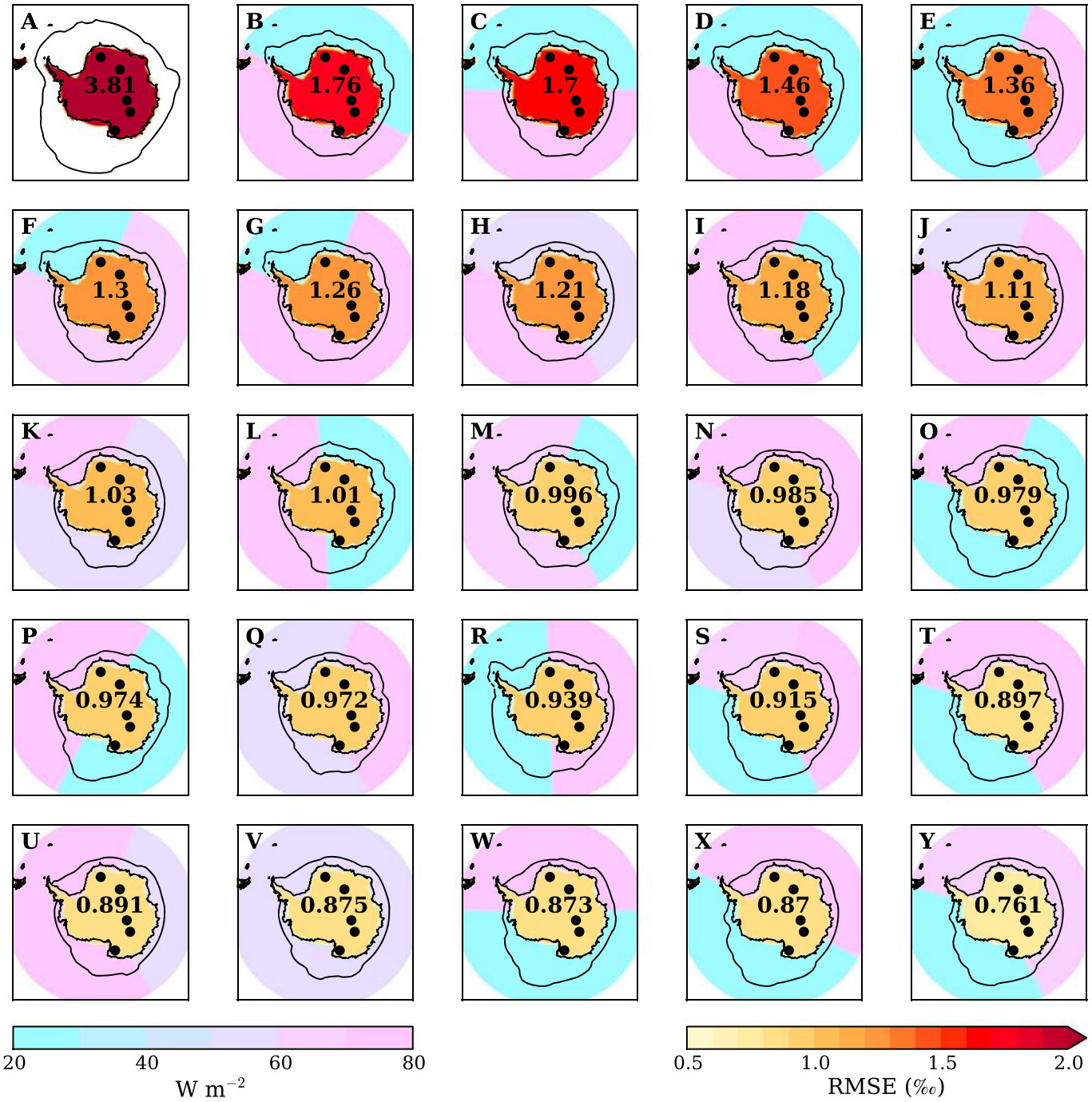

Figure 2. Model-data comparison for different magnitudes and spatial patterns of Antarctic sea ice retreat at 128 ka. Color shading of Antarctic mainland indicates the root-mean-square error (RMSE; rounded to three significant figures) between simulated $\delta^{18}O$ and observed $\delta^{18}O$ at five ice core sites (filled black circles). Panels are organized from (a) largest RMSE (least model-data agreement) to (y) smallest RMSE (best model-data agreement). Black contours signify the 15% September sea ice concentration threshold. Southern Ocean color shading shows the magnitude and spatial pattern of heat flux forcing (W m^{-2}) applied to sea ice in each experiment.

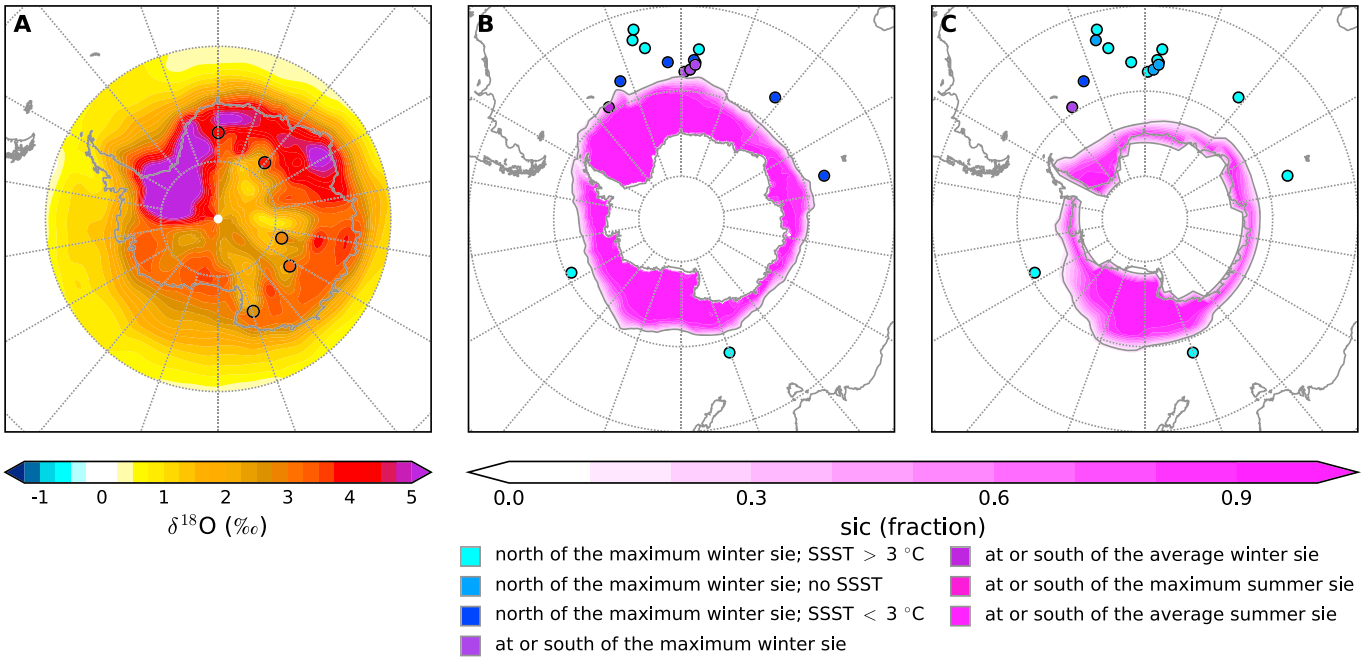

Figure 3. Antarctic winter sea ice extent at 128 ka and at present. (a) Spatial pattern of δ^{18}O anomalies (LIG-PI) in response to sea ice retreat that provides the best agreement with the δ^{18}O ice core data at 128 ka (filled circles). (b) Winter (September) sea ice fraction (mauve shading) and 15% concentration threshold (grey contour) from 1978 to 2013 satellite observations. (c) As in Figure 3b but for the simulated winter sea ice fraction from the LIG experiment that best agrees with the δ^{18}O ice core data at 128 ka, corresponding to Figure 3a. Filled circles in Figures 3b and 3c show the reconstructed sea ice extent (sie) and summer sea surface temperature (SSST) estimates, categorized using sea ice proxy data from marine sediment cores (see section 2), during the modern (Figure 3b) and the LIG (Figure 3c) sea ice minimum.

Second, the local evaporative input, warmer air temperatures, and shorter source-to-site distance increases the δ^{18}O composition of monthly precipitation. This tends to raise δ^{18}O. Since this latter effect dominates, the total change in δ^{18}O is positive.

3.2. Spatial Structure of the 128 ka Sea Ice Retreat

By simulating a range of different sea ice retreat scenarios, with varied magnitudes of retreat in the Atlantic, Pacific, and Indian sectors of the Southern Ocean, we aim to maximize the model-data agreement and provide insight into the most likely pattern of the 128 ka sea ice retreat. There is consistently model-data mismatch when greater sea ice retreat is applied to the Pacific sector (Figure 2). Greatest retreat in the Pacific sector results in the largest RMSE of this suite of experiments, exceeding 1.4‰ (Figure 2).

Model-data agreement improved with greater sea ice retreat in the Atlantic and Indian sectors. The lowest RMSE was achieved when equal sea ice retreat forcing was applied to the Atlantic and Indian sectors and weaker forcing was applied to the Pacific sector (Figure 2). This scenario led to a reduction in winter sea ice area of 67 and 59% in the Atlantic and Indian sectors, respectively, compared to 43% reduction in the Pacific sector, and a total reduction in Antarctic winter sea ice area of 54%. This scenario resulted in an improved spatial pattern of δ^{18}O anomalies (Figure 3a) and reduced the RMSE compared to the best fit uniform sea ice retreat scenario to 0.76‰.

All of the compiled marine LIG records exhibit intervals of peak SSSTs and/or minimum sea ice cover during the LIG (minimum ice and maximum temperature; MI-MT). The largest concentration of sites with SSST and sea ice reconstructions is located in the Atlantic sector of the Southern Ocean, where the MI-MT intervals consistently show that the mean winter sea ice limit was south of its modern position, while SSSTs of >3°C occurred close to the position of the modern winter sea ice limit (Figures 3b and 3c).

The two sites from the west and central Indian sector (PS2603-3 and MD 84 511) both record elevated SSSTs of >3°C during the MI-MT, while the westernmost and central Pacific sites (SO136-111 and PS58/271-1) are categorized with SSSTs > 3°C for both the modern and the MI-MT interval. Comparing the modern and reconstructed SSSTs revealed modest LIG increases of ~0.5°C in the westernmost Pacific and ~0.2°C in the central Pacific.

The reconstructions of oceanographic conditions during the MI-MT showed that the Atlantic sector experienced the greatest warming (likely corresponding with the largest southern shift in sea ice) relative to modern, while the least MI-MT warming (smallest southern shift of the sea ice edge) occurred in the Pacific sector. This circum-Antarctic pattern of MI-MT oceanographic conditions supports the modeled LIG distribution of mean winter sea ice cover, with the largest and smallest offsets between modern and modeled sea ice limits occurring in the Atlantic and Pacific sectors, respectively (Figures 3b and 3c).

4. Discussion

Our results indicate that there was significantly reduced winter sea ice extent in the Weddell Sea sector and around the East Antarctic coast at 128 ka. This finding agrees well with the interpretation of sea salt flux data (Schüpbach et al., 2013) and a compilation of LIG (sub-)Antarctic SSST records (Capron et al., 2014). The latter suggests an average Southern Ocean warming of approximately +2°C, with significant warming in the Atlantic and Indian sectors between 130 and 125 ka.

The bipolar-seesaw mechanism (Stocker & Johnsen, 2003), proposing that meltwater input into the North Atlantic from surrounding ice sheets leads to Northern Hemisphere cooling and Southern Hemisphere warming, is considered as the most likely explanation for the early timing of the LIG δ^{18}O maximum in Antarctica (Capron et al., 2014; Marino et al., 2015). Marino et al. (2015) give for the termination of North Atlantic meltwater input during the penultimate deglaciation an age of 130 $\pm$ 2 ka, which is roughly synchronous with the Antarctic isotope maximum.

Our results are consistent with this hypothesis, that meltwater input to the North Atlantic during the penultimate deglaciation led to prolonged weakening of the Atlantic Meridional Overturning Circulation (AMOC) and heat accumulation in the Southern Hemisphere. Warming was likely most intense in the South Atlantic due to the direct link with the AMOC and communicated to the Southern Ocean via the clockwise flowing Antarctic Circumpolar Current (ACC). The Atlantic warming was advected clockwise within the ACC, and consequently warming was concentrated in the Atlantic and Indian sectors of the Southern Ocean, leading to significant sea ice retreat in these two sectors, whereas minor warming in the Pacific sector resulted in less sea ice retreat there.

Marine-based sea ice reconstructions represent an independent line of evidence to support the Holloway, Sime, Singarayer, Tindall, Bunch, et al. (2016) Antarctic LIG sea ice retreat. LIG reconstructions based on marine records from the Southern Ocean are consistent with our model results, suggesting that the largest and smallest poleward shifts in the winter sea ice edge occurred in the Atlantic and Pacific sectors, respectively. However, no LIG marine records with published sea ice and/or SSST data are located sufficiently south of the modern sea ice edge to provide robust evidence of a major winter sea ice retreat. Consequently, we are unable to corroborate the proposed spatial structure of the LIG sea ice minimum, and only the development of sea ice and SSST reconstructions at sites closer to the continent will allow to sufficiently constrain the magnitude and geographical pattern of the LIG sea ice retreat.

In this study we isolate the isotopic response due only to changes in sea ice; the impact of Antarctic ice sheet elevation change is not investigated here. Since surface elevations in central East Antarctica may have varied within $\pm$200 m, with increased accumulation promoting mass gains and mass loss suggested due to increased melt (Bradley et al., 2013; Ritz et al., 2001), some elevation change may have contributed to the 128 ka isotopic change, potentially altering the magnitude of sea ice retreat required to explain the isotopic ice core data. However, the sign of elevation change at a given ice core site is uncertain and the magnitude of the resulting isotope anomaly is likely to be small relative to the total isotope change. This is because isotopic lapse rate calculations suggest that an elevation change of 200 m would relate to $\sim$1‰ change in δ^{18}O (Blisniuk & Stern, 2005; Poage & Chamberlain, 2001). Future work will aim to investigate, and better quantify, the relationship between ice sheet elevation changes and the Antarctic isotope record.

Our sea ice retreat scenario that shows the best agreement with the δ^{18}O anomalies observed in Antarctic ice cores at 128 ka predicts an annual mean sea ice area of roughly 8 million km^2, averaged over the whole simulation. This is compared to $\sim$19 million km^2 simulated in a preindustrial experiment. The corresponding best fit sea ice forcing is equal to a globally averaged heat input of 0.68 W m^{-2} or roughly 10% of the total radiative forcing of 6.7 W m^{-2} predicted in the representative concentration pathway 8.5 (RCP8.5) scenario

between 2000 and 2100 (IPCC, 2013). In this context, our spatially varying sea ice retreat scenario requires less additional heat input globally compared to that calculated previously by Holloway, Sime, Singarayer, Tindall, Bunch, et al. (2016), who assumed that the LIG sea ice retreat was uniform.

A dependence between outlet glacier terminus position and sea ice has been shown during the satellite record in Wilkes Land, East Antarctica (e.g., Miles et al., 2016, 2017, 2013). Reduced Antarctic sea ice and warmer Southern Ocean temperatures during the early LIG may have encouraged ice loss from marine basins in West and East Antarctica, contributing to the LIG sea level high stand of +6–9 m (Dutton et al., 2015; Kopp et al., 2009). However, although there is only one record with SSST estimates available from the central Pacific sector, we point out that the peak LIG proxy-derived warming reconstructed at this site of ~0.2°C above present (supporting information Table S1) is just 7–10% of the oceanic warming believed necessary for triggering a West Antarctic Ice Sheet (WAIS) collapse (Sutter et al., 2016), suggesting that sea water temperatures at this site remained below the threshold value for a WAIS collapse during the early LIG (e.g., Hillenbrand et al., 2002). However, lower SSST and sea ice retreat estimates from this sector may be equally consistent with input of relatively fresh glacial meltwater into the Pacific sector, caused by intensified WAIS melting at 128 ka (e.g., Holloway, Sime, Singarayer, Tindall, Bunch, et al., 2016).

Acknowledgments
This work was funded by NERC grants NE/P009271/1, NE/P013279/1, and NE/K004514/1. M. H. was also supported by the EPSRC-funded Past Earth Network (grant EP/M008363/1). E. W. is supported by a Royal Society Professorship. The data used are listed in the references, tables, and supporting information. Access to the Met Office Unified Model source code is available under license from the Met Office at http://www.metoffice.gov.uk/research/collaboration/um-collaboration. The climate model data are available on request from http://www.bridge.bris.ac.uk/resources/simulations.

References

Abram, N. J., Wolff, E. W., & Curran, M. A. J. (2013). A review of sea ice proxy information from polar ice cores. *Quaternary Science Reviews*, *79*, 168–183. https://doi.org/10.1016/j.quascirev.2013.01.011

Bakker, P., Masson-Delmotte, V., Martrat, B., Charbit, S., Renssen, H., Gröger, M., … Varma, V. (2014). Temperature trends during the present and last interglacial periods—A multi-model-data comparison. *Quaternary Science Reviews*, *99*, 224–243. https://doi.org/10.1016/j.quascirev.2014.06.031

Berger, A., & Loutre, M. F. (1991). Insolation values for the climate of the last 10 million years. *Quaternary Science Reviews*, *10*, 297–317.

Becquey, S., & Gersonde, R. (2002). Past hydrographic and climatic changes in the Subantarctic Zone of the South Atlantic—The Pleistocene record from ODP Site 1090. *Palaeogeography, Palaeoclimatology, Palaeoecology*, *182*(3–4), 221–239. https://doi.org/10.1016/S0031-0182(01)00497-7

Becquey, S., & Gersonde, R. (2003). A 0.55-Ma paleotemperature record from the Subantarctic zone: Implications for Antarctic Circumpolar Current development. *Paleoceanography*, *18*(1), 1014. https://doi.org/10.1029/2000PA000576

Benz, V., Esper, O., Gersonde, R., Lamy, F., & Tiedemann, R. (2016). Last Glacial Maximum sea surface temperature and sea-ice extent in the Pacific sector of the Southern Ocean. *Quaternary Science Reviews*, *146*, 216–237.

Bianchi, C., & Gersonde, R. (2002). The Southern Ocean surface between Marine Isotope Stages 6 and 5d: Shape and timing of climate changes. *Palaeogeography, Palaeoclimatology, Palaeoecology*, *187*, 151–177.

Blisniuk, P. M., & Stern, L. A. (2005). Stable isotope paleoaltimetry: A critical review. *American Journal of Science*, *305*(10), 1033–1074. https://doi.org/10.2475/ajs.305.10.1033

Bohrmann, G. (1999). Sedimentology of core PS2603-3 PANGAEA. In: Bohrmann, Gerhard; Kuhn, Gerhard (2011): Sedimentology on various cores from the South Atlantic. Dataset 760128. https://doi.org/10.1594/PANGAEA.54953

Bradley, S. L., Siddall, M., Milne, G. A., Masson-delmotte, V., & Wolff, E. (2013). Combining ice core records and ice sheet models to explore the evolution of the East Antarctic Ice sheet during the Last Interglacial period. *Global and Planetary Change*, *100*, 278–290.

Brathauer, U., & Abelmann, A. (1999). Late Quaternary variation in sea surface temperatures and their relationship to orbital forcing recorded in the Southern Ocean (Atlantic sector). *Paleoceanography*, *14*, 135–138.

Brathauer, U., Abelmann, A., Gersonde, R., Niebler, H.-S., & Fütterer, D. (2001). Calibration of Cycladophora davisiana events versus oxygen isotope stratigraphy in the subantarctic Atlantic Ocean—A stratigraphic tool for carbonate-poor Quaternary sediments. *Marine Geology*, *175*(1–4), 167–181.

Capron, E., Govin, A., Stone, E. J., Masson-Delmotte, V., Mulitza, S., Otto-Bliesner, B., … Eric, W. (2014). Temporal and spatial structure of multi-millennial temperature changes at high latitudes during the last interglacial. *Quaternary Science Reviews*, *103*, 116–133. https://doi.org/10.1016/j.quascirev.2014.08.018

Crosta, X., Pichon, J., & Burckle, L. H. (1998). Application of modern analog technique to marine Antarctic diatoms: Reconstruction of maximum sea-ice extent at the Last Glacial Maximum. *Paleoceanography*, *13*(3), 284–297. https://doi.org/10.1029/98PA00339

Crosta, X., Sturm, A., Armand, L., & Pichon, J.-J. (2004). Late Quaternary sea ice history in the Indian sector of the Southern Ocean as recorded by diatom assemblages. *Marine Micropaleontology*, *50*(3–4), 209–223. https://doi.org/10.1016/S0377-8398(03)00072-0

de Vernal, A., Gersonde, R., Goosse, H., Seidenkrantz, M. S., & Wolff, E. W. (2013). Sea ice in the paleoclimate system: The challenge of reconstructing sea ice from proxies—An introduction. *Quaternary Science Reviews*, *79*, 1–8. https://doi.org/10.1016/j.quascirev.2013.08.009

Deaney, E. L., Barker, S., & van de Flierdt, T. (2017). Timing and nature of AMOC recovery across Termination 2 and magnitude of deglacial CO_2 change. *Nature Communications*, *8*, 14595. https://doi.org/10.1038/ncomms14595

Dutton, A., Carlson, A., Long, A., Milne, G., Clark, P., DeConto, R., … Raymo, M. (2015). Sea-level rise due to polar ice-sheet mass loss during past warm periods. *Science*, *349*(6244), aaa4019. https://doi.org/10.1126/science.aaa4019

EPICA Community Members (2006). One-to-one coupling of glacial climate variability in Greenland and Antarctica. *Nature*, *444*(7116), 195–198. https://doi.org/10.1038/nature05301

Esper, O., & Gersonde, R. (2014a). New tools for the reconstruction of Pleistocene Antarctic sea ice. *Palaeogeography, Palaeoclimatology, Palaeoecology*, *399*, 260–283. https://doi.org/10.1016/j.palaeo.2014.01.019

Esper, O., & Gersonde, R. (2014b). Quaternary surface water temperature estimations: New diatom transfer functions for the Southern Ocean. *Palaeogeography, Palaeoclimatology, Palaeoecology*, *414*, 1–19. https://doi.org/10.1016/j.palaeo. 2014.08.008

Fischer, H., Fundel, F., Ruth, U., Twarloh, B., Wegner, A., Udisti, R., … Wagenbach, D. (2007). Reconstruction of millennial changes in dust emission, transport and regional sea ice coverage using the deep EPICA ice cores from the Atlantic and Indian Ocean sector of Antarctica. *Earth and Planetary Science Letters*, *260*(1–2), 340–354. https://doi.org/10.1016/j.epsl.2007.06.014

Frank, M., Gersonde, R., & Mangini, A. (1999). *Sediment redistribution, $^{230}Th_{ex}$-normalization and implications for the reconstruction of particle flux and export paleoproductivity* (pp. 409–426). Berlin, Heidelberg: Springer Berlin Heidelberg. https://doi.org/10.1007/978-3-642-58646-0_16

Frank, M., Gersonde, R., van der Loeff, M. R., Bohrmann, G., Nrnberg, C. C., Kubik, P. W., … Mangini, A. (2000). Similar glacial and interglacial export bioproductivity in the Atlantic sector of the Southern Ocean: Multiproxy evidence and implications for glacial atmospheric CO_2. *Paleoceanography*, *15*(6), 642–658. https://doi.org/10.1029/2000PA000497

Frank, M., Mangini, A., Gersonde, R., Rutgers van der Loeff, M., & Kuhn, G. (1996). Late Quaternary sediment dating and quantification of lateral sediment redistribution applying $^{230}Th_{ex}$: A study from the eastern Atlantic sector of the Southern Ocean. *Geologische Rundschau*, *85*(3), 554–566. https://doi.org/10.1007/BF02369010

Gersonde, R., & Ott, G. (1997). Stabile Isotope aus Sedimenten des Spätquartär vom Atlantisch-Indischen Rücken im Südpolarmeer, PANGAEA. In. Alfred Wegener Institute, Helmholtz Center for Polar and Marine Research, Bremerhaven, Dataset #772156.

Gersonde, R., & Zielinski, U. (2000). The reconstruction of late Quaternary Antarctic sea-ice distribution—The use of diatoms as a proxy for sea-ice. *Palaeogeography, Palaeoclimatology, Palaeoecology*, *162*(3–4), 263–286. https://doi.org/10.1016/S0031-0182(00)00131-0

Gersonde, R., Abelmann, A., Brathauer, U., Becquey, S., Bianchi, C., Cortese, G., … Fütterer, D. K. (2003). Last glacial sea surface temperatures and sea-ice extent in the Southern Ocean (Atlantic-Indian sector): A multiproxy approach. *Paleoceanography*, *18*(3), 1061. https://doi.org/10.1029/2002PA000809

Gersonde, R., Crosta, X., Abelmann, A., & Armand, L. (2005). Sea-surface temperature and sea ice distribution of the Southern Ocean at the EPILOG Last Glacial Maximum—A circum-Antarctic view based on siliceous microfossil records. *Quaternary Science Reviews*, *24*, 869–896. https://doi.org/10.1016/j.quascirev.2004.07.015

Goosse, H., Roche, D. M., Mairesse, a., & Berger, M. (2013). Modelling past sea ice changes. *Quaternary Science Reviews*, *79*, 191–206. https://doi.org/10.1016/j.quascirev.2013.03.011

Govin, A., Capron, E., Tzedakis, P. C., Verheyden, S., Ghaleb, B., Hillaire-Marcel, C., … Zahn, R. (2015). Sequence of events from the onset to the demise of the last interglacial: Evaluating strengths and limitations of chronologies used in climatic archives. *Quaternary Science Reviews*, *129*, 1–36. https://doi.org/10.1016/j.quascirev.2015.09.018

Hillenbrand, C.-D., Fütterer, D. K., Grobe, H., & Frederichs, T. (2002). No evidence for a Pleistocene collapse of the West Antarctic Ice Sheet from continental margin sediments recovered in the Amundsen Sea. *Geo-Marine Letters*, *22*, 51–59. https://doi.org/10.1007/s00367-002-0097-7

Hodell, D. A., Charles, C. D., Curtis, J. H., Mortyn, P. G., Ninnemann, U. S., & Venz, K. A. (2003). Data report: Oxygen isotope stratigraphy of ODP Leg 177 Sites 1088, 1089, 1090, and 1094. In R. Gersonde, D. Hodell, & P. Blum (Eds.), *Proceedings of the Ocean Drilling Program, Scientific Results Leg 177* (pp. 1–26). Texas: Ocean Drilling Program, College Station.

Hoffman, J. S., Clark, P. U., Parnell, A. C., & He, F. (2017). Regional and global sea-surface temperatures during the last interglaciation. *Science*, *355*(6322), 276–279. https://doi.org/10.1126/science.aai8464

Holloway, M., Sime, L., Singarayer, J., Tindall, J., Bunch, P., & Valdes, P. (2016). Antarctic last interglacial isotope peak in response to sea ice retreat not ice-sheet collapse. *Nature Communications*, *7*, 12293. https://doi.org/10.1038/ncomms12293

Holloway, M. D., Sime, L. C., Singarayer, J. S., Tindall, J. C., & Valdes, P. J. (2016). Reconstructing paleosalinity from $\delta^{18}O$: Coupled model simulations of the Last Glacial Maximum, Last Interglacial and Late Holocene. *Quaternary Science Reviews*, *131*, 350–364. https://doi.org/10.1016/j.quascirev.2015.07.007

Intergovernmental Panel on Climate Change (IPCC) (2013). *Climate change 2013: The physical science basis. Contribution of Working Group I to the Fifth Assessment Report of the Intergovernmental Panel on Climate Change*. New York: Cambridge University Press.

Jouzel, J., Masson-Delmotte, V., Cattani, O., Dreyfus, G., Falourd, S., Hoffmann, G., … Wolff, E. W. (2007). Orbital and millennial Antarctic climate variability over the past 800,000 years. *Science*, *317*(5839), 793–796. https://doi.org/10.1126/science.1141038

Kawamura, K., Parrenin, F., Lisiecki, L., Uemura, R., Vimeux, F., Severinghaus, J. P., … Watanabe, O. (2007). Northern Hemisphere forcing of climatic cycles in Antarctica over the past 360,000 years. *Nature*, *448*(7156), 912–916. https://doi.org/10.1038/nature06015

Kopp, R. E., Simons, F. J., Mitrovica, J. X., Maloof, A. C., & Oppenheimer, M. (2009). Probabilistic assessment of sea level during the last interglacial stage. *Nature*, *462*(7275), 863–867. https://doi.org/10.1038/nature08686

Levine, J., Yang, X., Jones, A., & Wolff, E. (2014). Sea salt as an ice core proxy for past sea ice extent: A process-based model study. *Journal of Geophysical Research: Atmospheres*, *119*, 5737–5756. https://doi.org/10.1002/2013JD020925

Liu, X., & Battisti, D. S. (2015). The influence of orbital forcing of tropical insolation on the climate and isotopic composition of precipitation in South America. *Journal of Climate*, *28*(12), 4841–4862. https://doi.org/10.1175/JCLI-D-14-00639.1

Loulergue, L., Schilt, A., Spahni, R., Masson-Delmotte, V., Blunier, T., Lemieux, B., … Chappellaz, J. (2008). Orbital and millennial-scale features of atmospheric CH_4 over the past 800,000 years. *Nature*, *453*(7193), 383–6. https://doi.org/10.1038/nature06950

Mackensen, A. (2001). Oxygen and carbon stable isotope tracers of Weddell Sea water masses: New data and some paleoceanographic implications. *Deep Sea Research Part I: Oceanographic Research Papers*, *48*(6), 1401–1422. https://doi.org/10.1016/S0967-0637(00)00093-5

Marino, G., Rohling, E. J., Rodréguez-Sanz, L., Grant, K. M., Heslop, D., Roberts, A. P., … Yu, J. (2015). Bipolar seesaw control on last interglacial sea level. *Nature*, *522*(7555), 197–201. https://doi.org/10.1038/nature14499

Masson-Delmotte, V., Buiron, D., Ekaykin, A., Frezzotti, M., Gallée, H., Jouzel, J., … Vimeux, F. (2011). A comparison of the present and last interglacial periods in six Antarctic ice cores. *Climate of the Past*, *7*(2), 397–423. https://doi.org/10.5194/cp-7-397-2011

Miles, B. W. J., Stokes, C. R., & Jamieson, S. S. R. (2016). Pan-ice-sheet glacier terminus change in East Antarctica reveals sensitivity of Wilkes Land to sea-ice changes. *Science Advances*, *2*(5), e1501350. https://doi.org/10.1126/sciadv.1501350

Miles, B. W. J., Stokes, C. R., & Jamieson, S. S. R. (2017). Simultaneous disintegration of outlet glaciers in Porpoise Bay (Wilkes Land), East Antarctica, driven by sea ice break-up. *The Cryosphere*, *11*, 427–442. https://doi.org/10.5194/tc-11-427-2017

Miles, B. W. J., Stokes, C. R., Vieli, A., & Cox, N. J. (2013). Rapid, climate-driven changes in outlet glaciers on the Pacific coast of East Antarctica. *Nature*, *500*(7464), 563–566. https://doi.org/10.1038/nature12382

Moore, J. K., Abbott, M. R., & Richman, J. G. (1999). Location and dynamics of the Antarctic polar front from satellite sea surface temperature data. *Journal of Geophysical Research*, *104*(C2), 3059–3073. https://doi.org/10.1029/1998JC900032

Mulitza, S., Arz, H., Kemle-von Mücke, S., Moos, C., Niebler, H.-S., Pätzold, J., & Segl, M. (1999). *The South Atlantic carbon isotope record of planktic foraminifera* (pp. 427–445). Berlin, Heidelberg: Springer Berlin Heidelberg. https://doi.org/10.1007/978-3-642-58646-0_17

Niebler, H. (1995). Reconstruction of paleo-environmental parameters using stable isotopes and faunal assemblages of planktonic foraminifera in the South Atlantic Ocean (Reports on Polar Research 167). Bremerhaven: Alfred Wegener Institut for Polar and Marine Research.

Niebler, H.-S. (2004). Distribution of planktic foraminifera, factor analysis, SST of sediment core PS2498-1. Department of Geosciences, Bremen University, PANGAEA, https://doi.org/10.1594/PANGAEA.55887

Noone, D., & Simmonds, I. (2004). Sea ice control of water isotope transport to Antarctica and implications for ice core interpretation. *Journal of Geophysical Research*, *109*, D07105. https://doi.org/10.1029/2003JD004228

Nürnberg, C. C., Bohrmann, G., Schlüter, M., & Frank, M. (1997). Barium accumulation in the Atlantic sector of the Southern Ocean: Results from 190,000-year records. *Paleoceanography*, *12*(4), 594–603. https://doi.org/10.1029/97PA01130

Parrenin, F., Barnola, J., Beer, J., Blunier, T., Castellano, E., Chappellaz, J., … Fujita, S. (2007). The EDC3 chronology for the EPICA Dome C ice core. *Climate of the Past*, *3*, 485–497.

Petit, J. R., Jouzel, J., Raynaud, D., Barkov, N. I., Barnola, J.-M., Basile, I., … Stievenard, M. (1999). Climate and atmospheric history of the past 420,000 years from the Vostok ice core, Antarctica. *Nature*, *399*, 429–436.

Pichon, J.-J., Labeyrie, L. D., Bareille, G., Labracherie, M., Duprat, J., & Jouzel, J. (1992). Surface water temperature changes in the high latitudes of the Southern Hemisphere over the last glacial-interglacial cycle. *Paleoceanography*, *7*(3), 289–318. https://doi.org/10.1029/92PA00709

Poage, M. A., & Chamberlain, C. P. (2001). Empirical relationships between elevation and the stable isotope composition of precipitation and surface waters: Considerations for studies of paleoelevation change. *American Journal of Science*, *301*(1), 1–15.

Pugh, R. S., McCave, I. N., Hillenbrand, C. D., & Kuhn, G. (2009). Circum-Antarctic age modelling of Quaternary marine cores under the Antarctic Circumpolar Current: Ice-core dust-magnetic correlation. *Earth and Planetary Science Letters*, *284*(1–2), 113–123. https://doi.org/10.1016/j.epsl.2009.04.016

Ritz, C., Rommelaere, V., & Dumas, C. (2001). Modeling the evolution of Antarctic ice sheet over the last 420,000 years: Implications for altitude changes in the Vostok region. *Journal of Geophysical Research*, *106*(D23), 31,943–31,964. https://doi.org/10.1029/2001JD900232

Roche, D., Crosta, X., & Renssen, H. (2012). Evaluating Southern Ocean sea-ice for the Last Glacial Maximum and pre-industrial climates: PMIP-2 models and data evidence. *Quaternary Science Reviews*, *56*, 99–106. https://doi.org/10.1016/j.quascirev.2012.09.020

Schneider-Mor, A., Yam, R., Bianchi, C., Kunz-Pirrung, M., Gersonde, R., & Shemesh, A. (2005). Diatom stable isotopes, sea ice presence and sea surface temperature records of the past 640 ka in the Atlantic sector of the Southern Ocean. *Geophysical Research Letters*, *32*, L10704. https://doi.org/10.1029/2005GL022543

Schneider-Mor, A., Yam, R., Bianchi, C., Kunz-Pirrung, M., Gersonde, R., & Shemesh, A. (2008). Nutrient regime at the siliceous belt of the Atlantic sector of the Southern Ocean during the past 660 ka. *Paleoceanography*, *23*, PA3217. https://doi.org/10.1029/2007PA001466

Schneider-Mor, A., Yam, R., Bianchi, C., Kunz-Pirrung, M., Gersonde, R., & Shemesh, A. (2012). Variable sequence of events during the past seven terminations in two deep-sea cores from the Southern Ocean. *Quaternary Research*, *77*, 317–325.

Schüpbach, S., Federer, U., Kaufmann, P. R., Albani, S., Barbante, C., Stocker, T. F., & Fischer, H. (2013). High-resolution mineral dust and sea ice proxy records from the Talos Dome ice core. *Climate of the Past*, *9*(6), 2789–2807. https://doi.org/10.5194/cp-9-2789-2013

Schurer, A. P., Tett, S. F. B., & Hegerl, G. C. (2014). Small influence of solar variability on climate over the past millennium. *Nature Geoscience*, *7*(2), 1–5. https://doi.org/10.1038/ngeo2040

Sime, L. C., Tindall, J. C., Wolff, E. W., Connolley, W. M., & Valdes, P. J. (2008). Antarctic isotopic thermometer during a CO_2 forced warming event. *Journal of Geophysical Research*, *113*, D24119. https://doi.org/10.1029/2008JD010395

Sime, L. C., Wolff, E. W., Oliver, K. I. C., & Tindall, J. C. (2009). Evidence for warmer interglacials in East Antarctic ice cores. *Nature*, *462*, 342–345. https://doi.org/10.1038/nature08564

Spahni, R., Chappellaz, J., Stocker, T. F., Loulergue, L., Hausammann, G., Kawamura, K., … Jouzel, J. (2005). Atmospheric methane and nitrous oxide of the late Pleistocene from Antarctic ice cores. *Science*, *310*(5752), 1317–1321. https://doi.org/10.1126/science.1120132

Stenni, B., Buiron, D., Frezzoti, M., Albani, S., Barbante, C., Bard, E., … Udisti, R. (2011). Expression of the bipolar see-saw in Antarctic climate records during the last deglaciation. *Nature Geoscience*, *4*(1), 46–49. https://doi.org/10.1038/ngeo1026

Stocker, T. F., & Johnsen, S. J. (2003). A minimum thermodynamic model for the bipolar seesaw. *Paleoceanography*, *18*(4), 1087. https://doi.org/10.1029/2003PA000920

Sutter, J., Gierz, P., Grosfeld, K., Thoma, M., & Lohmann, G. (2016). Ocean temperature thresholds for last interglacial west Antarctic ice sheet collapse. *Geophysical Research Letters*, *43*, 2675–2682. https://doi.org/10.1002/2016GL067818

Tindall, J. C., Valdes, P. J., & Sime, L. C. (2009). Stable water isotopes in HadCM3: Isotopic signature of El Niño–Southern Oscillation and the tropical amount effect. *Journal of Geophysical Research*, *114*, D04111. https://doi.org/10.1029/2008JD010825

Waelbroeck, C., Paul, A., Kucera, M., Rosell-MelÃ, A., Weinelt, M., Schneider, R., … Turon, J. L. (2009). Constraints on the magnitude and patterns of ocean cooling at the Last Glacial Maximum. *Nature Geoscience*, *2*, 127–132. https://doi.org/10.1038/ngeo411

Wolff, E. W., Barbante, C., Becagli, S., Bigler, M., Boutron, C. F., Castellano, E., … Wegner, A. (2010). Changes in environment over the last 800,000 years from chemical analysis of the EPICA Dome C ice core. *Quaternary Science Reviews*, *29*, 285–295. https://doi.org/10.1016/j.quascirev.2009.06.013

Wolff, E. W., Fischer, H., Fundel, F., Ruth, U., Twarloh, B., Littot, G., … Gaspari, V. (2006). Southern Ocean sea-ice extent, productivity and iron flux over the past eight glacial cycles. *Nature*, *440*(7083), 491–496. https://doi.org/10.1038/nature04614

Zielinski, U., Bianchi, C., Gersonde, R., & Kunz-Pirrung, M. (2002). Last occurrence datums of the diatoms Rouxia leventerae and Rouxia constricta: Indicators for marine isotope stages 6 and 8 in Southern Ocean sediments. *Marine Micropaleontology*, *46*(1–2), 127–137.

Zielinski, U., Gersonde, R., Sieger, R., & Fütterer, D. (1998). Quaternary surface water temperature estimations: Calibration of a diatom transfer function for the Southern Ocean. *Paleoceanography*, *13*(4), 365–383. https://doi.org/10.1029/98PA01320